

Development and Initial Testing of the Tiltrotor Test Rig

C. W. Acree, Jr.
Aeromechanics Office
NASA Ames Research Center
Moffett Field, California

A. L. Sheikman
Aeromechanics Office
NASA Ames Research Center
Moffett Field, California

Abstract

The NASA Tiltrotor Test Rig (TTR) is a new, large-scale prop rotor test system, developed jointly with the U.S. Army and Air Force, to develop a new, large-scale prop rotor test system for the National Full-Scale Aerodynamics Complex (NFAC). The TTR is designed to test advanced prop rotors up to 26 feet in diameter at speeds up to 300 knots, and even larger rotors at lower airspeeds. This combination of size and speed is unprecedented and is necessary for research into 21st-century tiltrotors and other advanced rotorcraft concepts. The TTR will provide critical data for validation of state-of-the-art design and analysis tools.

Notation

ATB	Advanced Technology Blades
DCMS	Drive Control Monitoring System
JHL	U. S. Army Joint Heavy Lift
JVX	Joint Vertical Experimental prop rotor
NFAC	National Full-Scale Aerodynamics Complex
OARF	Outdoor Aerodynamic Research Facility
PTR	Prop Test Rig
RTA	Rotor Test Apparatus
TTR	Tiltrotor Test Rig
A	Rotor disk area
c	Rotor chord (thrust weighted)
C_P	Power coefficient, $P/\rho A V_t^3$
C_T	Thrust coefficient, $T/\rho A V_t^2$
M_{tip}	Tip Mach number
N	Number of blades
Q	Dynamic pressure, $\frac{1}{2} \rho V^2$
R	Rotor radius
T	Rotor thrust
V	Wind tunnel airspeed
V_t	Rotor tip speed
Ω	Rotor speed, rpm
ρ	Atmospheric density
σ	Rotor solidity, $Nc/\pi R$

Introduction

The Tiltrotor Test Rig (TTR) was developed by NASA to fill a test capability gap for large-scale prop rotors in high-speed axial flight up to 300 knots and tiltrotor conversion mode up to 180 knots. The TTR can also test in hover up to 30,000 lb rotor thrust and in helicopter mode (edgewise flight) up to 150 knots. The TTR is designed for use in the National Full-Scale Aerodynamics Complex (NFAC) at NASA Ames Research Center.

Presented at the AHS International 74th Annual Forum & Technology Display, Phoenix, Arizona, May 14-17, 2018. This is a work of the U.S. Government and is not subject to copyright protection in the U.S.

Development of the Tiltrotor Test Rig originated during the U. S. Army Joint Heavy Lift (JHL) program as a collaborative effort between the Army and NASA. Sizing studies were initiated in 2007, resulting in a NASA contract to Bell Helicopter and Triumph Aerospace Systems Newport News (now Calspan) to design and manufacture the TTR and supporting equipment. The TTR was effectively complete by January of 2015, when calibration of the rotor balance began. The TTR was installed in the NFAC in March 2017.

The TTR is a horizontal axis rig and rotates on the test-section turntable to face the rotor into the wind at high speed (300 knots), or fly edgewise at low speed (150 knots), or at any angle in between (Fig. 1). The TTR can accommodate a variety of rotors. A 26-ft diameter checkout rotor (Fig. 2) is installed for the initial wind tunnel test.



Fig. 1. TTR in the NFAC 40- x 80-ft test section, oriented in airplane mode (0 deg yaw).

The goal of the TTR effort is to provide the capability to test large-scale prop rotors at full NFAC operational speeds. The primary objective of the first test entry is to fully check out the TTR, including integration with the NFAC. Rotor test data will be collected primarily as a means to that end, although every opportunity will be used to collect rotor performance and loads data for research.



Fig. 2. 26-ft diameter TTR checkout rotor.

This paper describes the TTR hardware, the checkout rotor, the combined system instrumentation, and key development activities in preparation for the first test in the NFAC. A brief history of previous large-scale prop rotor tests is included. Important TTR development activities are covered in Refs. 1-3; those efforts are summarized and updated here. While the focus is on describing the design and technical capabilities of the TTR, selected test data are presented to show demonstrated capabilities.

Brief History of Prop rotor Testing at the NFAC

NASA has a long history of testing large-scale (25-ft or larger) prop rotors in the NFAC. A few such research programs are mentioned below because their data and experience will inevitably be compared with that of the TTR.

Two direct ancestors of the TTR are the Propeller Test Rig of the 1970s (Fig. 3) and the Prop Test Rig of the 1980s (Figs. 4 and 5), both of which were used in multiple tests of isolated prop rotors (Refs. 4-11). Installed power of the Propeller Test Rig was 3000 hp and the rotor tilted vertically about the horizontal axis. Although vertical tilt matched the XV-15 aircraft in conversion mode, the rotor was placed closer to the test section ceiling than desirable.



Fig. 3. Bell XV-15 rotor on the Propeller Test Rig (1970).



Fig. 4. Scaled JVX rotor on the Prop Test Rig (1991).

In contrast, the Prop Test Rig (PTR) rotated horizontally on the wind tunnel turntable to mimic tiltrotor conversion. The PTR was also used at the Outdoor Aerodynamic Research Facility (OARF) at Ames for hover testing (Fig. 5). The OARF tests were free of wall effects but were dependent on weather for near-zero wind conditions. The PTR was used for over 20 years; tests included XV-15, ATB, and JVX proprotors. The ATB and JVX rotors were alternative blades fitted to the XV-15 hub; see Refs. 8 and 12 for descriptions of the ATB rotor, and Refs. 9-13 for the JVX rotor. The ATB rotor was also flown on the XV-15 (Ref. 14). The JVX rotor was designed as a 0.685-scale V-22 rotor, although the V-22 rotor evolved significantly during subsequent development.



Fig. 5. ATBs on the Prop Test Rig at the OARF (1984).

Another series of full-scale rotor tests utilized the Dynamic Test Stand (a.k.a. Dynamic Wing Test Stand), which was a dynamically scaled, semi-span wing with nacelle. There were multiple variants intended for aeroelastic stability tests with different rotors (Figs. 6 and 7). Tests in the early 1970s included the Bell Model 300 and Boeing Model 222 rotors (Refs. 4 and 15, respectively), competitors for the XV-15 research aircraft.

Although not strictly in the line of development toward the TTR, the Rotor Test Apparatus (RTA) bears mentioning because it was used to test the XV-15 rotor in hover and helicopter mode (Ref. 16). The RTA is limited to 3000 hp and edgewise flight at moderate airspeeds.



Fig. 6. XV-15 rotor on the Dynamic Test Stand (1970).



Fig. 7. Boeing 222 semi-span wing and rotor (1972).

The most remarkable outcome of these tests is that the data remain valuable, and in some cases unequalled, over 40 years later. Unfortunately, none of the high-speed rigs survive. The need for a new, more capable facility for testing 21st-century proprotors prompted the development of the TTR.

Hardware Description

The wind tunnel, test stand, checkout rotor, and auxiliary equipment are described in this section. As this is the first wind-tunnel entry of the TTR, emphasis is placed on describing its functionality and capability.

NFAC Wind Tunnel

The TTR was designed specifically for operations in the NFAC and relies on the facility for power, cooling water, and other utilities, including research data acquisition. The NFAC is located at Ames Research Center (Fig. 8) and managed and operated by the U.S. Air Force's Arnold Engineering Development Center.

The TTR checkout test is currently underway in the NFAC 40- by 80-foot test section. The wind tunnel has a closed circuit with an oblong test section 39 ft high, 79 ft wide, and 80 ft long. The maximum test section velocity is approximately 300 knots (currently limited to about 240 knots, pending upgrades to the fan drives). The tunnel walls are treated with 6 in of acoustically absorbent material to reduce reflections that can contaminate the noise field.

The NFAC can be internally reconfigured as an open-circuit tunnel with an 80- by 120-ft rectangular test section. The TTR can be tested in the 80x120, although at much lower airspeed (about 100 knots maximum).



Fig. 8. National Full-Scale Aerodynamics Complex (NFAC)

TTR Technical Details

Table 1 summarizes the dimensions and technical features of the TTR. The airspeed limits apply to the TTR under ideal conditions; wind-tunnel operations are limited by dynamic

pressure, not velocity. 0-deg yaw is airplane mode, with the rotor pointing into the wind (Fig. 1), and 90-deg yaw (counter-clockwise, looking up) is helicopter mode. For reference, the TTR and the checkout rotor are assigned Bell Model No. 699.

Table 1. TTR Dimensions and Design Capabilities

Length, including spinner	435 in
Width, main nacelle only	85 in
Width, including pylons	140 in
Depth, main nacelle only	67 in
Weight, including rotor	60,800 lb
Rotor hub position:	
fwd of balance center	88 in
height above floor (40x80)	234 in
Power, max design	6,000 hp
Power, max qualified (30 min)	5,500 hp
Power, continuous (2 hr)	5,000 hp
Rotor shaft speed, max	629.5 rpm
Max airspeed, 0-deg yaw	300 knots (305 lb/ft ²)*
Max airspeed, 90-deg yaw	180 knots (110 lb/ft ²)*

*40x80 limit=262 lb/ft², 80x120 limit=33 lb/ft²

The TTR has a three-strut layout to interface with the test section turntable (Fig. 1). The mounting struts attach directly to the test section T-frame, a rotating structure underneath the floating turntable. The T-frame was modified to rotate ± 180 deg from its normal orientation to accommodate the TTR. The large overhang between the single forward strut and the rotor provides space for a semi-span wing, as would be needed for wing/rotor interference measurements. (No wing was installed for the current entry; Refs. 9-11 describe earlier tests with the PTR and a wing.)

For maximum accuracy, rotor forces and moments are measured by a dedicated balance installed between the gearbox and the rotor. Rotor torque is measured by an instrumented torque tube inside the gearbox. The balance and its calibration are described in detail in the Instrumentation and Rotor Balance Calibration sections of this report.

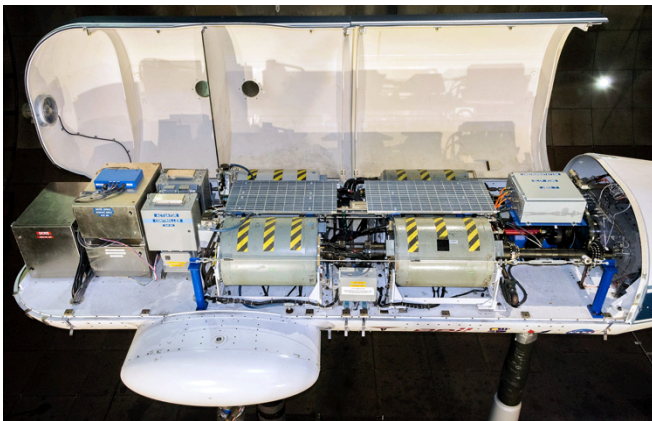
Table 2 summarizes the capability of the current balance. The TTR structure is sized for even higher loads: $\pm 20,000$ lb shear, $\pm 90,000$ ft-lb hub moment, and 75,000 ft-lb torque. These loads are intended for proprotor hubs with substantial hub moments, based on emerging new tiltrotor concepts. However, such loads will require a new rotor balance. Calibrated accuracy is discussed in the Rotor Balance Calibration section.

Figure 9 shows the TTR main deck with upper cowlings open. The four large cylinders are the drive motors; the various boxes are all electronics cabinets. The aft end of the gearbox is just visible under the cowling.

Table 2. Rotor Balance Capability (max range)

Load (applied at the rotor hub)	Limit
Normal force (thrust), lb	30,000
In-plane shear, lb	$\pm 10,000$
Hub moment, ft-lb	$\pm 60,000$
Torque, ft-lb	72,000
Actuator loads, lb	$\pm 11,000$

The water-cooled, AC induction motors are powered in pairs by two NFAC motor-generator sets, rated up to 150 Hz, or 3000 rpm nominal, and 1100 Volts. The TTR motors are presently rated to 5000 hp total continuous power—enough to drive proprotors far more capable than any currently in existence at this scale. Typically only one pair of motors is powered during testing of the checkout rotor. The drive train was designed to allow operation down to 20% of maximum speed, which is a new technology area for efficient tiltrotor designs.

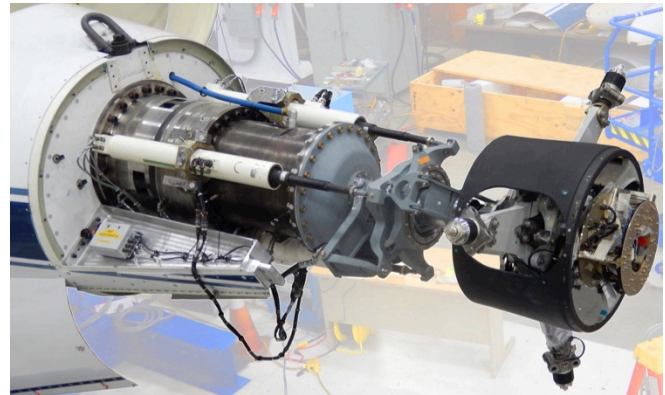
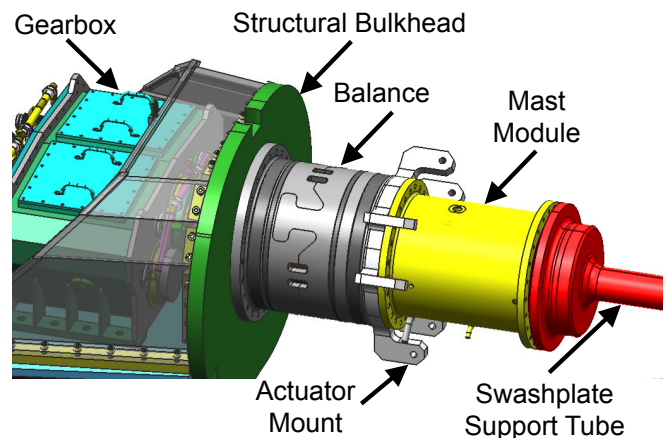
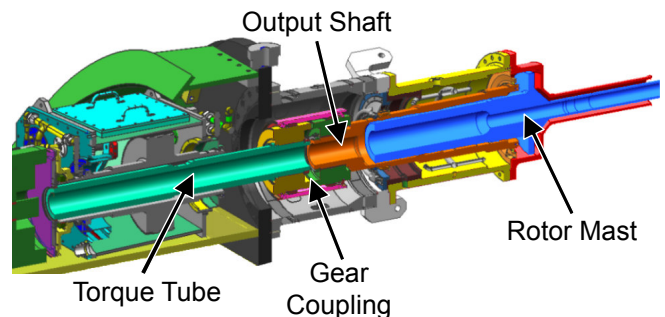
**Fig. 9. TTR main deck: drive motors and electronics.**

The TTR gearbox and drive train are sized for 6000 hp. The drive motors were surplus units refurbished and upgraded to TTR requirements. The four motors are theoretically capable of providing 1500 hp each, but there was no readily available facility that could bench test the TTR motors to full speed and torque at rated voltage, current, and frequency. The TTR itself is the means of qualifying the motors to full power. Motor testing is therefore an important part of the first entry and a good example of the unique challenges faced by TTR development.

To facilitate testing different rotors, TTR has a multi-component drive train. The terminology used here is the “rotor mast” is the component that connects directly to the rotor hub. Installing a different rotor usually requires a different hub, hence a different rotor mast. If the mast were an integral part of the drive train, a new rotor would require a new drive train, including a modified gearbox. To facilitate testing different rotors, the TTR has an innovative drive train that transfers rotor loads to the rotor balance via a mast module. The mast module has a hollow drive shaft that accepts a splined rotor mast. This arrangement allows the rotor mast and hub to be removed and replaced without

disassembling the rest of the drive train or disturbing the balance or gearbox. The various components of this system are briefly described here.

The forward end of the TTR—from the gearbox bulkhead to the rotor instrumentation hat—is shown in Fig. 10 (here without fixed cowlings, spinner or pitch links). For clarity, external and internal drawings are shown in Figs. 11 and 12. The rotor balance attaches directly to the TTR main bulkhead, and the mast module and control actuators attach to the forward end of the balance. The swashplate support tube attaches to the forward end of the mast module. A torque tube, gear coupling, drive shaft, and rotor mast all run through the center of the balance/mast module/support-tube assembly. All rotor instrumentation is routed through the “hat” inside the spinner.

**Fig. 10. TTR forward end: rotor balance, mast module, controls, hub and skirt fairings.****Fig. 11. TTR gearbox, rotor balance, and mast module.****Fig. 12. TTR drive train internal components.**

Checkout Test Rotor

To reduce risk, the initial checkout test uses a rotor based on a flight-proven design. The rotor was built specifically for NASA by Bell, derived from the right-hand rotor of the Leonardo AW609. Although built in the same blade molds as the production rotor, the checkout rotor is unique: it has no deicing or pendulum absorbers, and has special instrumentation and modified controls as appropriate for a wind-tunnel test article. The pitch horn lugs are inverted to connect to the TTR control system. These modifications prevent the rotor from ever being flown on an aircraft.

Figure 2 shows the checkout rotor, including protective epoxy strips for blade instrumentation. Figure 10 shows the control system and partially exposed rotor hub, and Fig. 13 is an exploded view of the hub and blade. Table 3 summarizes the rotor characteristics.

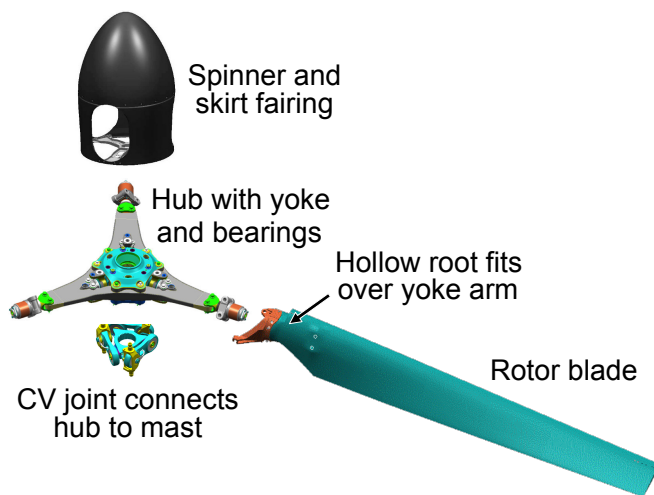


Fig. 13. Checkout rotor exploded view (components not to scale).

Table 3. TTR Checkout Rotor Characteristics

Number of blades	3
Diameter	26.0 ft
Disc area (per rotor)	530.9 ft ²
Solidity (thrust weighted)	0.0908
Blade chord (thrust weighted)	14.83 in
Blade area (per rotor)	48.2 ft ²
Blade twist (non-linear)	47.5 deg
Blade planform	linear taper
Blade tip shape	square
100% rotor speed (helicopter mode)	569 rpm
Tip speed	775 ft/sec
84% rotor speed (airplane mode)	478 rpm
Tip speed	651 ft/sec
Collective range*	61.5 deg
Gimbal limit (flapping stop)	±11 deg
Precone	2.75 deg
Undersling	0.36 in
Delta-3	-15 deg
Direction of rotation (looking aft)*	CCW

*As installed on TTR.

The rotor is a stiff-in-plane design with a gimballed hub; there are no discrete flap or lag hinges. The rotor hub has three arms, or yokes, that carry inner and outer pitch bearings (Fig. 13), with centrifugal (CF) bearings at each end. The hub is mounted to the rotor mast by a gimbal, so that all blades flap together: if one quadrant flaps up, the opposite flaps down. The gimbal is a constant velocity (CV) joint and includes a flapping spring. The hub spring and rotor bearings are all elastomeric units.

The rotor blades have hollow roots that slip over the yokes and bearings. The entire hub, including pitch links, pitch horns, and blade roots, is covered by a spinner and side panels, or skirts, all of which rotate together. The skirts have oversize cutouts to allow for blade flapping.

The rotor control system uses a conventional rise-and-fall swashplate, here driven by three long-stroke, dual-motor, electric jackscrew actuators. Total actuator travel is 17 in, equivalent to 61.5 deg of blade pitch for the checkout rotor. The large amount of pitch motion is required for a proprotor that must operate over an extremely large range of inflow velocities (0-300 knots).

Operator controls are provided by a pair of identical control consoles that provide fully redundant backup in case of failure. Each console has a set of conventional collective and cyclic controls, plus individual actuator controls. Each console has a pair of displays with critical rotor information.

A companion console, the Drive Control Monitoring System (DCMS), controls essentially everything on the TTR except the rotor itself. The DCMS controls and monitors only low-rate systems. The rotor can be safely flown down from full speed and power to a stop even after a complete failure of the DCMS. Controls for the NFAC motor-generators (M-G sets) that drive the motors are co-located with the DCMS.

The rotor control consoles and DCMS are completely independent of the NFAC data system, although the two systems can exchange data.

Instrumentation

Table 4 summarizes the instrumentation currently installed on the TTR and checkout rotor. A few measurement categories unique to the TTR are discussed below. The rotor balance is discussed in a separate subsection, Rotor Loads Measurement. In addition, the NFAC data system acquires a comprehensive set of wind tunnel test conditions, including yaw angle, airspeed, temperature, density, static pressure, etc.

Tables 5 through 9 give more details of the TTR instrumentation. The tables are organized as traditional rotating and nonrotating sensors, with additional details for blade strain gages, the rotor balance system, and external microphones. A few categories overlap; e.g., the torque tube is in Tables 5 and 8.

Table 4. TTR Instrumentation Summary

68 Rotating Channels:
Blade and yoke strain gages
Hub flap, blade pitch
Pitch link loads
Mast torque and bending
Elastomeric bearing temperatures
Spinner loads
Torque-tube loads and temperatures
88 Fixed Channels:
Control positions & loads
Swashplate guide tube bending
Rotor balance loads and temperatures
Strut loads
Microphones
Separate system for TTR utilities

Table 5. Rotating System Instrumentation (strain gages unless otherwise noted).

Blade	12
Yoke & spindles ^a	8 (4 locations)
Pitch links	3
Hub flap angle	2 axes
Blade pitch angle	2 blades
Mast torque ^b	3 (2 locations)
Mast bending	6 (2 axes at 3 locations)
Torque tube	8
Swashplate & driver loads	2
Swashplate temperature	2
Hub spring temperature	4
CF bearing temperature	2 blades
Spinner ^c	12 (4 locations)
Hub accelerometers ^d	3
Hub pressure ^d	1

^aOne yoke arm and its bearing spindles have beam and chord gages at two locations each.

^bMast torque has a backup gage at only one location.

^cAll three spinner upper support arms (the ones closest to the end of the mast) have a full set of beam/chord/torsion gages. Only one lower support arm has a full set.

^dThe hub accelerometers and pressure sensor are mounted to the instrumentation plate, just above the hub. The plate does not flap with the hub.

Table 6. Blade Strain Gages

Station	Beam	Chord	Torsion
0.21 R	x	x	
0.37 R	x	x	
0.45 R	x	x	x
0.58 R	x	x	
0.75 R	x	x	x

Table 7. Nonrotating System Instrumentation

Rotor balance system (all sensors)	56
Control actuator loads	3
Control actuator positions ^a	6
Swashplate anti-drive load	1
Swashplate support tube strain gages	2
Shaft encoders ^b	2
Mast module pressure	1
Support strut strain gages ^c	12
Microphones	4
Low-speed anemometer ^d	1

^aEach control actuator has primary and backup LVDTs.

^bEach shaft encoder outputs 4096/rev plus a 1/rev reference.

^cEach support strut has two pairs of transverse strain gages (primary and backup).

^dThe low-speed anemometer is installed only for hover.

TTR has four data streams: rotor research data, safety of flight data, acoustics data, and utility data. Rotating-system data passes through a conventional, multi-channel slip ring before being digitized. The research data are acquired by the NFAC data system (Ref. 17, with 24-bit A/D converters. The data are oversampled then digitally resampled at even fractions of the N/rev pulse train. Most of the data are resampled and stored at 256/rev; acoustics data are sampled at 2048/rev (>20 kHz at 569 rpm). Safety of flight data are processed via a separate data stream, sampling at 2 kHz.

A separate, on-board system manages low-rate utility data, such as cooling water temperature, lubrication oil, and balance temperature. This data stream primarily feeds the rotor operator displays and controls (DCMS and control console).

Selected Rotor Instrumentation Details

In addition to the traditional blade and pitch-link strain gages, there are separate hub flap and blade pitch transducers. In principal, hub flapping (gimbal tilt angle, two axes), blade pitch, and swashplate position (collective and cyclic) together constitute an overdetermined system of measurements: 8 sensors and 5 degrees of freedom. TTR has redundant transducers for safety and for improved accuracy.

Spinner loads can be significant in airplane mode (150+ knots), or even at moderate speed in helicopter mode, where the spinner is edgewise to the flow. Concerns that spinner loads might be nonlinear and difficult to distinguish from rotor loads led to TTR having a system for directly measuring spinner loads. The spinner and skirt fairings are supported by spokes that allow loads to bypass the rotor hub and gimbal (Fig. 14). The spokes are strain gaged to directly measure spinner loads. Spinner data are discussed in the section Aerodynamic Tares.

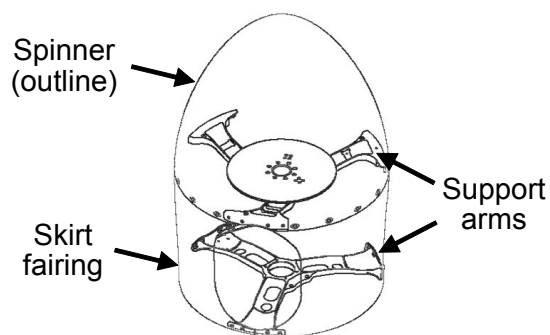


Fig. 14. Spinner (outline) and support arms.

The rotor balance does not measure aerodynamic loads on the TTR nonrotating cowl and fairings. Furthermore, the TTR is too heavy for the 40x80 scales, so traditional methods for measuring aerodynamic tares cannot be used. The mounting struts (Fig. 1) must react cowl, rotor, and spinner loads, plus their own drag loads. The struts were therefore strain gaged and calibrated in situ prior to the installation of the TTR. The strut data are not as accurate as the scale data, but are nevertheless adequate for safety-of-flight loads monitoring.

Rotor Loads Measurement

The TTR has a balance and torque tube that work together to measure all rotor loads, including actuator loads. The balance measures net rotor and actuator loads except torque, which is measured by the torque tube. The torque tube connects to the output shaft via a gear coupling that transfers only torque, isolating the torque tube from bending and thrust loads. The torque tube has a diaphragm coupling to relieve stresses arising from thermal expansion.

Table 8. Balance & Torque Tube

Balance strain gages	24
Balance temperatures	24
Torque tube strain gages	2
Torque tube temperatures	2
Diaphragm coupling strain gages	2
Diaphragm coupling temperatures	2

The balance (Table 8) is a metal cylinder fixed to the gearbox bulkhead. Rotor loads are transferred to the balance via thrust bearings inside the mast module (Fig. 11). For accurate measurement, loads are concentrated at four machined posts, each with two sets of three strain gages (axial, side, and normal). The balance has thermal isolation rings and a temperature control system, including pre-heating, with metric and ground temperature sensors every 45 deg.

The torque tube (Fig. 12) has strain gages mounted to a necked section for high sensitivity. The diaphragm coupling also has strain gages to measure any residual thrust. The torque tube and diaphragm coupling have primary and secondary (backup) measurements.

For a proprotor at high speed, control loads can be a very large component of total thrust, so care must be taken to measure such loads. The control actuators mount to the TTR via gimbals, which transmit only axial loads from the rotor. The gimbals in turn mount directly to the metric side of the balance, so that the balance measures the sum of rotor thrust through the rotor mast and control loads through the actuators. The control actuators (nonrotating) and pitch links (rotating) have calibrated strain gages to measure control loads.

The entire rotor loads measurement system is commonly referred to as the “rotor balance”, or just “balance”. The name derives from traditional wind-tunnel scales that balance loads being measured against known weights. The Wright brothers invented a purely aerodynamic balance for their wind tunnel. TTR does everything electronically, but honors the traditional name.

TTR Development

The TTR design contract was awarded to Bell in July 2009. Various components were constructed and delivered to NASA in stages, beginning in April 2012. Pre-operational activities included refurbishment of the drive motors, drive system spin tests, and construction of a calibration rig. After installation in the NFAC, activities included a ground vibration test (shake test) and rotor-off tests to acquire aerodynamic tare data. This section describes the major activities between completion of the rig and acquisition of rotor data, namely balance calibration, shake testing, strut calibration, and rotor-off tare tests.

Rotor Balance Calibration

The entire rotor loads measurement system, including balance and torque tube, must be calibrated when installed on the TTR to account for flexing under load. A calibration rig (cal rig) was designed and built specifically for TTR; Figs. 15 and 16 show the TTR cal rig. For clarity, Fig. 17 illustrates the calibration hardware without the supporting structure.



Fig 15. TTR Calibration Rig.

For calibration, the rotor was replaced by metric hardware, the most prominent component of which was a large steel crossbeam (Figs. 17 and 18). Loads were applied by a set of 11 actuators and load tubes, plus a chain-and-sprocket system for mast torque. Applied loads were measured by in-line load cells. To react calibration torque loads, the torque tube was grounded at the aft end of the gearbox.



Fig. 16. TTR installed in the Calibration Rig, with metric hardware in place of the rotor.

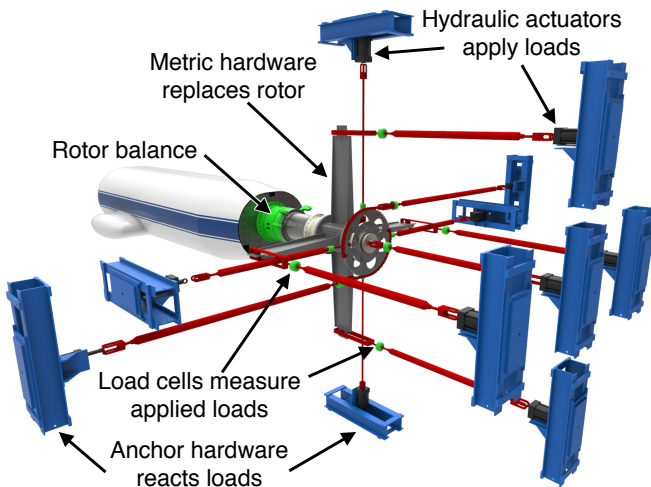


Fig. 17. Calibration hardware (exploded view).

Photogrammetry techniques were used to ensure proper alignment of applied loads during calibration. 2920 retroreflective photogrammetry targets were installed in various places on the TTR, cal rig, and load hardware; a subset of the targets is visible in Fig. 18. A pair of specialized cameras tracked the movement of the targets under load. Reference 1 describes the technique in detail and provides additional details of calibration procedures.

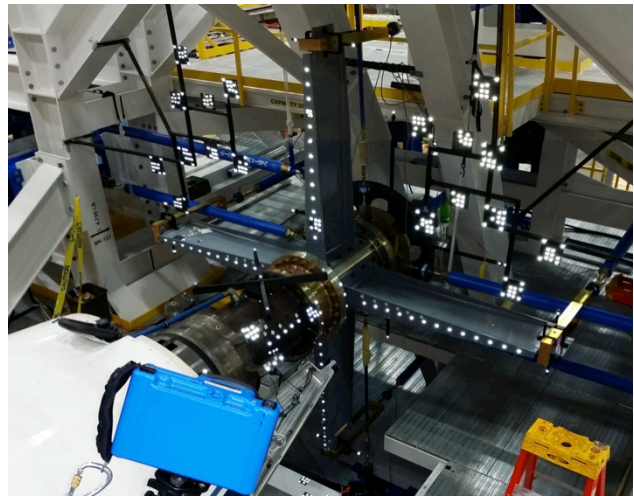


Fig. 18. Photogrammetry camera (blue box in foreground) and retroreflective targets (white dots.)

The calibration of the TTR was complicated by several considerations, some unique to TTR. These considerations are outlined below, along with the calibration approach used to address them.

- 1) The TTR rotor balance was oversized for the checkout rotor. Also, the rotor has a gimballed hub, so it cannot sustain large moments. Calibration was therefore conducted over two load ranges: the full load range of the rotor balance (Table 2), and the load range for the checkout rotor (Table 10). The maximum rotor thrust is just over 1/2 of the balance range, maximum hub moments are only 1/8 of the balance range, and maximum torque is less than 1/3 of the torque tube range.
- 2) For a proprotor, the ratio of thrust in cruise to that in hover is approximately the inverse of the aircraft lift-to-drag ratio, yet the torque can be equally high. Hence thrust can vary by an order of magnitude depending on flight condition. The balance must be sized for hover loads, which presents major challenges for maintaining good accuracy in airplane mode. The result is that accuracy in thrust is worse than in any other axis.
- 3) There are two primary rotor load paths: the rotor shaft and the control system. Those loads are reacted by the mast module and torque tube. In addition, transverse swashplate loads are reacted by the swashplate support tube, which is grounded to the mast module. However, calibration of the balance and torque tube does not depend on the exact load path through the control system, so the actuators and pitch links were disconnected during the balance calibration.
- 4) The rotor mast cannot sustain full-range balance loads, so two different configurations of the metric hardware were required. The standard configuration applied all loads to the rotor mast up to the limits of Table 10, and a second configuration applied full-range shear loads and moments (Table 2) directly to the mast module, bypassing the rotor mast.

Table 10. Rotor Balance Calibration for Checkout Rotor Loads.

Hub Load	Range	2 σ Error*	2 σ / Range
Normal force (thrust)	15,248 lb	120 lb	0.79 %
In-plane horizontal	$\pm 8,250$ lb	24 lb	0.15 %
In-plane vertical	$\pm 8,250$ lb	16 lb	0.10 %
Hub moment, vertical axis	$\pm 7,500$ ft-lb	159 ft-lb	0.11 %
Hub moment, horizontal	$\pm 7,500$ ft-lb	202 ft-lb	0.13 %
Torque	22,338 ft-lb	46 ft-lb	0.21 %

*Loads are applied at the hub, but accuracy is calculated at the balance.

In addition, there were a few diagnostic configurations to check weight tares and torque-tube lockout effects. The resulting calibration effort was equivalent to at least two traditional rotor balance calibrations. The scope of the effort can be suggested by enumerating a few items:

- 4153 load combinations during calibration
- 2²⁸ strain-gage combinations for data analysis
- 2⁷² coefficient combinations in the calibration equations

The load combinations include all directions and magnitudes tested; the strain-gage combinations include both primary and secondary (backup) gages; and the coefficient combinations assume every possible combination of strain gages without physical constraints.

In practice, the reduced-range calibration (Table 10) was analyzed as a subset of the full range (Table 2). Most of the strain-gage combinations for the rotor balance and torque tube can be eliminated by physical considerations, and nearly all of the coefficient combinations can be eliminated by mathematical considerations. For example, at least 6 balance gages and 2 torque-tube gages are required, which eliminates over 100 million possibilities. The effort required to determine the optimum calibration is nevertheless daunting.

Table 10 summarizes the calibration accuracy for the best set of calibration equations derived to date. Accuracy in most axes is good, 0.21% range or less. However, thrust accuracy is 0.79% of range. This result is disappointing but not surprising, given that the rotor balance is working over barely 50% of its design range. Re-optimizing the calibration data specifically for low thrust may give a slight improvement to measurement accuracy in airplane mode.

In high-speed axial flight (airplane mode), the pitch links carry a very large fraction of total thrust. Pitch-link loads are reacted by the swashplate, control actuators, and ultimately the balance. The pitch links and actuators have calibrated strain gages to measure control system loads.

Dynamics, Including Shake Test

The checkout rotor is stiff-in-plane (it has no lead-lag hinges), therefore it is immune to ground resonance. However, when operating as a propeller in high-speed axial flow, the rotor/TTR system is susceptible to whirl flutter.

Proper calculation of the stability boundary is essential and requires accurate modeling or measurement of the TTR's modal response to dynamic load inputs. That is, it is necessary to construct a mathematical model of the TTR's structural dynamics without a rotor, then to couple that model to a dynamic model of the rotor.

Dynamics modeling and analyses can be summarized as follows: (1) initial Bell predictions of stability, based on nominal rotor and structural properties; (2) a shake test to acquire data for the TTR as installed in the NFAC; and (3) updated stability predictions by NASA, based on the shake test data (frequencies, damping, and mode shapes).

A NASTRAN model of the TTR, mounting struts, and 40x80-ft test section T-frame was created to provide pre-test modal predictions. Bell coupled a model of the TTR to a model of the T-frame provided by the NFAC. The combined model was subsequently updated by NASA to include as-built weight and c.g. data, plus other modifications to better represent the TTR, mounting struts, etc. as installed.

The load path from the T-frame to the fixed NFAC structure varies slightly with yaw angle, so there were in practice three different NASTRAN models, at 0-, 45-, and 90-deg yaw angles. The mode shapes and frequencies were coupled to a rotor model with the comprehensive analysis code CAMRAD II (Ref. 18). Coupled dynamic behavior was analyzed at a variety of flight conditions matched to yaw angle, yielding predictions of aeroelastic stability.

Even small errors in a NASTRAN model can lead to large errors in stability predictions. NASTRAN cannot predict structural damping in any case. Therefore, an extensive shake test program was carried out to verify NASTRAN predictions of mode shapes and frequencies, and to provide damping data (Ref. 2).

Figures 19 and 20 show just two of the 16 configurations tested. In addition to three yaw angles, loads were input into three locations: a dummy hub, and forward and aft lifting lugs. The lifting lugs allowed the excitation loads to bypass the hub and rotor mast, with the intent of achieving better coupling between the shaker and the TTR main structure. Reference 2 describes the procedure in detail, including data analysis and results.



Fig. 19. Shake test with lateral input at the rotor hub.

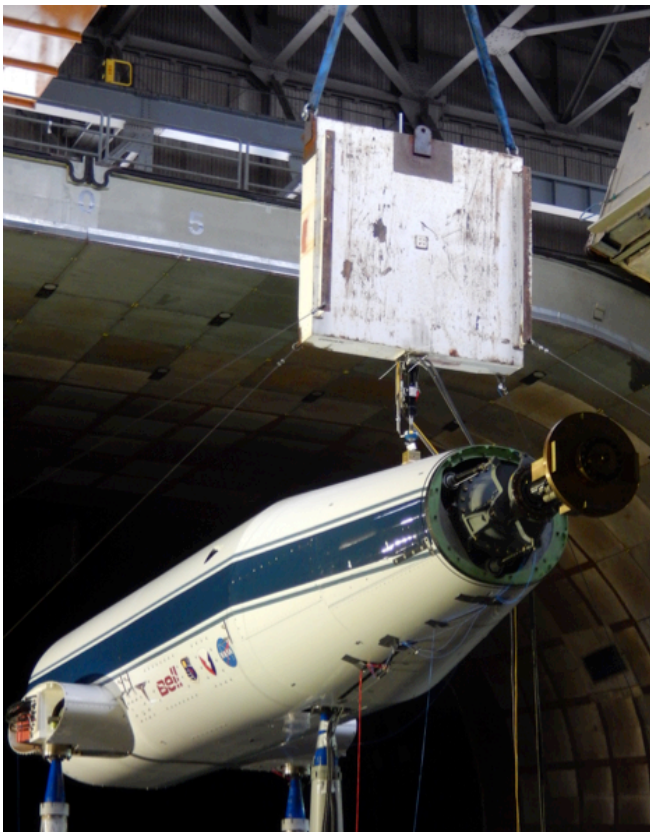


Fig. 20. Shake test with vertical input at the forward lifting lug.

Using both the NASTRAN predictions and experimentally determined dynamics, the TTR is predicted to be stable beyond 400 knots (Ref. 3). In hover, the checkout rotor is predicted to be stable until well into stall, at power levels beyond the capability of the rig.

Strut Deflection Measurements

The three mounting struts each have strain gages to measure loads in the horizontal plane, perpendicular to the vertical axis of each strut. Before the TTR was installed in the NFAC, the struts were calibrated in place, two at a time, by loading them against each other. Photogrammetry was used to measure the deflections of the struts under load.

The shake test revealed that the predicted and measured frequencies did not always match well. The availability of photogrammetry data allowed for more extensive diagnostics of the NASTRAN model than is usually possible. The photogrammetry data revealed that the struts deflected more than predicted at the base, where they attach to the T-frame. The NASTRAN model was accordingly revised to better represent the local structure. (The results of Ref. 3 are based on experimental data and remain definitive.)

Although not critical for the first entry of the TTR, the updated NASTRAN model of the NFAC support structure will be of value to future tests of models and rigs other than TTR. This is an example of the unexpected, serendipitous value of the TTR development effort

Aerodynamic Tares

Spinner loads can be a significant fraction of the total loads measured by the balance. Careful attention must therefore be paid to collecting good aerodynamic tare data for the spinner. This section describes some of the challenges faced during acquisition and interpretation of spinner tare data.

The spinner and skirts are held in place by two sets of support arms, upper and lower (Fig. 14). Only the upper set is fixed to the mast; the lower set is free to slide up or down along the mast. Hence the lower support transfers only transverse forces to the mast; the upper support reacts the axial forces. The supports, spinner and skirts can be installed without the hub, blades or pitch links.

The TTR provides two sets of measurements to help determine spinner tares. These include direct measurement of spinner loads as well as rotor balance measurements. Reliability of direct spinner measurements is unproven, and spinner tare forces are at the limits of rotor balance accuracy. Analysis of TTR checkout test data will evaluate the adequacy of each set of measurements.

The spinner supports have strain gages to measure bending loads, hence spinner drag. The strain gages can collectively measure axial loads, but are poorly placed to measure transverse loads and moments.

The proper setup for measuring spinner tares poses a dilemma, in that neither a blades-off nor hub-off configuration can provide the exact flow conditions that would exist if the blades had no aerodynamic effect on the spinner. The hub yokes and bearings are covered by the blade roots, which act as aerodynamic fairings extending inside the spinner skirts. Two exposed yokes can be seen protruding from the skirt fairing in Fig. 10.

Removing the blades would expose the yokes flatwise to the flow and create high-drag flow conditions not present during normal operations. If instead the entire hub were to be removed, the flow disturbance caused by the yokes would not exist, but the effective area of the holes in the skirt fairing would be much larger than with blades installed, again resulting in non-representative flow conditions.

Given that there is no perfect way to acquire spinner tare data, it was decided to simulate an ideal spinner by fairing over the skirt holes. This is the cleanest possible configuration, hence the lowest spinner drag. Figure 21 shows the fully-faired spinner and skirts at multiple yaw angles.



Fig. 21. Multiple exposure of spinner tare measurements, 0-100 deg yaw.

The rotor balance is vented, so pressure is equalized between the metric and non-metric sides. In principal, no pressure corrections should be needed for spinner or balance load measurements. Nevertheless, a pressure transducer was installed at the front face of the mast module for diagnostic purposes.

Tare data were taken at 0-deg yaw up to 275 knots, and at several yaw angles from 0 to 100 deg up to 155 knots (Fig. 21). All data reported here were taken with the spinner turning at normal shaft speeds.

Initial data analysis suggests that spinner drag at 0-deg yaw, 578 rpm is 0.26 ft² with holes covered, and highly linear with Q . The maximum axial load is less than the nominal balance accuracy (Table 10). Analysis is continuing, so further effort may result in revised estimates of drag. Similar analyses are underway for transverse drag in helicopter mode.

Rotor Testing

The primary goal of the first wind tunnel test is to demonstrate the safe and effective operation of the TTR. It is emphasized that acquiring rotor research data, while highly desirable, is not the critical objective of the test. Nevertheless, extensive research data will be a natural fallout of TTR envelope expansion. Operating limits are usually set by the rotor, not by the TTR itself.

The major objectives of the first entry are prioritized as follows:

1. Demonstrate the operational capability of the TTR throughout its design flight envelope.
2. Acquire data to support upgrades to the TTR as needed to improve safety and productivity.
3. Acquire benchmark rotor data to determine research capability.
4. Acquire rotor data unique to the 40x80 test section (> 100 knots).

Rotor research objectives of the first entry are:

1. Fully characterize hub/spinner drag
2. Hover up to rotor thrust limit (stall)
3. Airplane mode (axial flow) up to maximum tunnel speed
4. Helicopter mode (edgewise flow) up to 120 knots
5. Conversion mode up to 180 knots

Reference 19 gives details of the checkout rotor's flight envelope, from which the wind tunnel test conditions were derived (Fig. 22). Nominal test points are near the middle of the conversion corridor. The rotor can be flown at low speeds with a slight negative tilt angle, useful for descent to landing, so the figure contains a few test points to simulate such flight conditions. Not shown in the figure are airplane-mode (0-deg nacelle angle) flight conditions beyond 180 knots up to the maximum speed of the NFAC. In a wind tunnel, there is no need to trim the complete aircraft, so the boundaries of Fig. 22 are not necessarily definitive for an isolated rotor on the TTR.

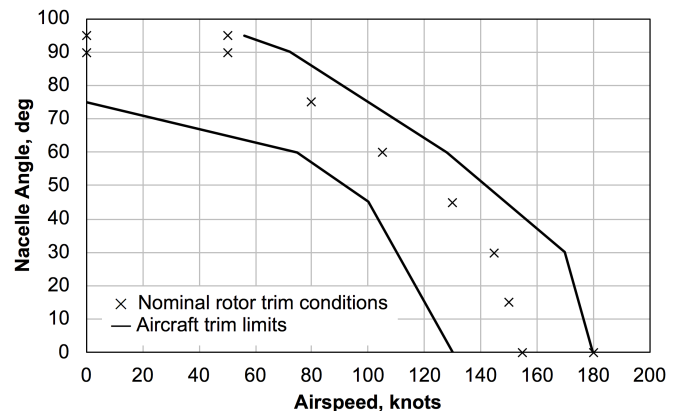


Fig. 22. Nominal rotor conversion corridor (Ref. 19); airspeeds >180 knots not shown.

Rotor Test Data

As of the date of publication of this paper, only a limited amount of hover data have been acquired. The results are summarized below.

In the NFAC, true hover is challenging at full scale. The effects of tunnel walls cannot be completely avoided in the 40x80 test section. Furthermore, the rotor's induced velocity continues around the tunnel circuit without completely dissipating, so the test conditions are actually low-speed vertical climb.

Data taken to date include limited hover conditions at 569 rpm (helicopter-mode tip speed). The data presented here were taken with the rotor facing downstream (180 deg yaw) and NFAC vane sets 6 and 7 open, which minimized flow through the tunnel circuit. For the thrust sweeps in Figs. 23-25, $\Omega=569.2\pm1.1$ rpm and $M_{tip}=0.683\pm0.001$.

Maximum thrust was limited by control-system loads. The critical rotor controls are aircraft parts and are designed for trimmed flight loads, not the more severe conditions possible in a wind tunnel. Revised operational techniques are being considered that may raise the achievable thrust. Even with the current limits, the data show that the TTR itself is not a limiting factor in collecting rotor performance data.

Figure 23 plots power versus thrust, and Fig. 24 plots the resulting circuit flow velocity, equivalent to vertical rate of climb. Here the velocity is measured as normal test section airspeed (in this case, negative with respect to the test section, but plotted positive with respect to the rotor). To give a sense of scale, the data of Fig. 23 are replotted in Fig. 26 in physical units. The power vs. thrust data show excellent repeatability, even with considerable scatter in the induced flow velocity.

To provide more accurate measurements of circuit flow velocity, additional hover tests are planned to include a low-speed anemometer upstream of the rotor.

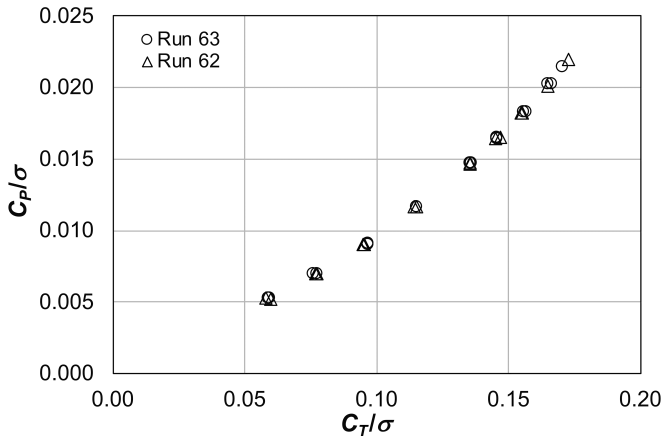


Figure 23. Power vs. thrust at 569 rpm, 180-deg yaw, near-hover conditions (rotor coefficients).

The data acquired to date allow a few conclusions:

1. The TTR can drive and control the checkout rotor in near-hover conditions without issues.
2. The rotor can be operated without limitations due to the test stand or integration with the NFAC.
3. The instrumentation is adequate, including the rotor balance.

Rotor-off tares, including spinner data, are currently being evaluated. Plans for the immediate future include high-speed axial flow (airplane mode) tests up to maximum wind tunnel velocity, followed by testing in helicopter and conversion mode.

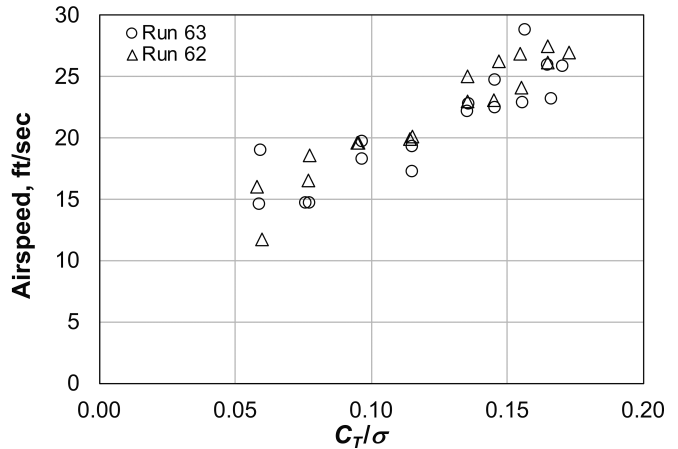


Figure 24. Vertical climb velocity vs. thrust at 569 rpm, 180-deg yaw.

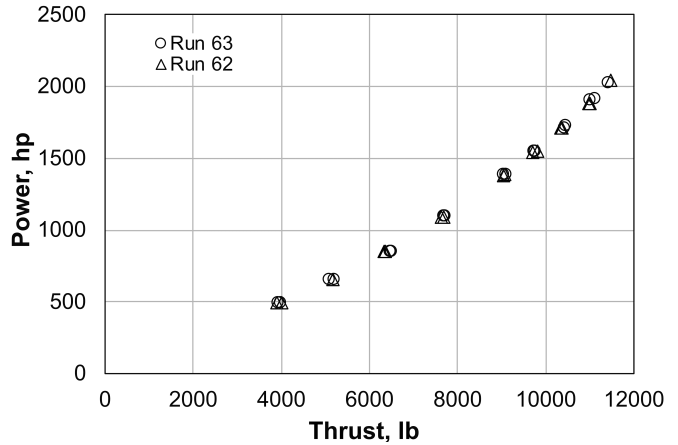


Figure 25. Power vs. thrust at 569 rpm, 180-deg yaw, near-hover conditions (physical units).

Concluding Remarks

A new, full-scale rotor test capability, the Tiltrotor Test Rig (TTR), has advanced to wind-tunnel testing, now underway. Achievements to date include:

1. Construction of the TTR, including refurbishment of the drive motors.

2. Calibration of the rotor balance system, including construction of a calibration rig, multiple-load-path calibration, and data analysis.
3. Extensive ground vibration tests (shake tests), demonstrating acceptable frequency placement.
4. Acquisition of aerodynamic tare data (rotor off) up to 275 knots in airplane mode, and during yaw sweeps from 0 to 100 deg up to 155 knots.
5. Initial near-hover (low-speed vertical climb) tests.

Plans include extended hover testing, then airplane, helicopter, and conversion modes.

Author contact: C. W. Acree cecil.w.acree@nasa.gov
A. L. Sheikman alex.l.sheikman@nasa.gov

Acknowledgements

The authors wish to acknowledge the efforts of the TTR test team in preparing the TTR for testing and for doing their utmost to ensure a successful entry. Special acknowledgement is made to the NFAC test directors, Chris Hartley and William Bartow, for their expertise and dedication. Susan Gorton (NASA) and Tom Wood (Bell) deserve thanks for their unfailing support, often behind the scenes. Many of the graphics and photographs were provided by Eduardo Solis.

The authors feel particularly obliged to acknowledge the contributions of Wel-Chong “Ben” Sim, who sadly passed away before the test could be completed.

References

- ¹Solis, E., and Meyn, L., “Photogrammetric Deflection Measurements for the Tiltrotor Test Rig (TTR) Multi-Component Rotor Balance Calibration,” American Helicopter Society Technical Meeting on Aeromechanics Design for Vertical Lift, San Francisco, California, January 20-22, 2016.
- ²Russell, C.R., and Acree, C.W., “Modal Test and Analysis of the NASA Tiltrotor Test Rig,” American Helicopter Society Technical Conference on Aeromechanics Design for Transformative Vertical Lift, San Francisco, CA, January 16-19, 2018.
- ³Kottapalli, S., and Acree, C.W., “Analytical Performance, Loads, and Aeroelastic Stability of a Full-Scale Isolated Proprotor,” American Helicopter Society Technical Conference on Aeromechanics Design for Transformative Vertical Lift, San Francisco, CA, January 16-19, 2018.
- ⁴Bell Helicopter Company, “Advancement of Proprotor Technology. Task II – Wind-Tunnel Test Results,” NASA CR-114363, Bell Report 300-099-004, Sept. 1971.
- ⁵Marr, R. L., “Wind Tunnel Test Results of 25-Ft. Tilt Rotor During Autorotation,” NASA CR-137824; Bell Report 301-099-005; February 1976.
- ⁶Felker, F. F., Betzina, M. D., and Signor, D. B., “Performance and Loads Data from a Hover Test of a Full-Scale XV-15 Rotor,” NASA TM-86833, November 1985.
- ⁷Felker, F. F., Young, L. A., and Signor, D. B., “Performance and Loads Data from a Hover Test of a Full-Scale Advanced Technology XV-15 Rotor,” NASA TM-86854, January 1986.
- ⁸Bartie, K., Alexander, H., McVeigh, M., La Mon, S., and Bishop, H., “Hover Performance Tests of Baseline Metal and Advanced Technology Blade (ATB) Rotor Systems for the XV-15 Tilt Rotor Aircraft,” NASA CR-177436, October 1986.
- ⁹Felker, F. F., Signor, D. B., Young, L. A., and Betzina, M. D., “Performance and Loads Data From a Hover Test of a 0.658-Scale V-22 Rotor and Wing,” NASA TM-89419, April 1987.
- ¹⁰Felker, F. F., Shinoda, P. R., Heffernan, R. M., and Sheehy, H. F., Wing Force and Surface Pressure Data from a Hover Test of a 0.658-Scale V-22 Rotor and Wing. NASA TM-102244, Feb. 1990.
- ¹¹Felker, F. F., “Results from a Test of a 2/3-Scale V-22 Rotor and Wing in the 40- by 80-Foot Wind Tunnel,” American Helicopter Society 47th Annual Forum, Phoenix, Arizona, May 1991.
- ¹²Alexander, H. R., Maisel, M. D., and Giulianetti, D. J., The Development of Advanced Technology Blades for Tiltrotor Aircraft. Paper No. 39, 11th European Rotorcraft Forum, London, England, Sept. 1985.
- ¹³Farrell, M. K., “Aerodynamic Design of the V-22 Osprey Proprotor,” American Helicopter Society 45th Annual Forum, Boston, Massachusetts, May 1989.
- ¹⁴Wellman, B., “Advanced Technology Blade Testing on the XV-15 Tilt Rotor Research Aircraft,” American Helicopter Society 48th Annual Forum, Washington, D. C., June 1992.
- ¹⁵Magee, J. P., and Alexander, H. R., “Wind Tunnel Tests of a Full Scale Hingeless Prop/Rotor Designed for the Boeing Model 222 Tilt Rotor Aircraft,” NASA CR 114664, October 1973.
- ¹⁶Light, J. S., “Results from an XV-15 Rotor Test in the National Full-Scale Aerodynamics Test Complex,” American Helicopter Society 53rd Annual Forum, Virginia Beach, Virginia, April-May 1997.

¹⁷van Aken, J. and Yang, L., “Development of a new State-of-the-Art Data Acquisition System for the National Full-Scale Aerodynamics Complex Wind Tunnels,” AIAA-2009-1346, 47th AIAA Aerospace Sciences Meeting, Orlando, FL, January 2009.

¹⁸Johnson, W., “Technology Drivers in the Development of CAMRAD II,” American Helicopter Society Aeromechanics Specialists Conference, San Francisco, CA, January 19-21, 1994.

¹⁹Harris, J.C., Scheidler, P.F, Hopkins, R, and Fortenbaugh, R.L., “Initial Power-Off Testing of the BA609 Tiltrotor,” American Helicopter Society 66th Annual Forum Proceedings, Phoenix, AZ, May 11-13, 2010.